

# Lipid rafts in C6 glioma cell line: role in the regulation of calcium signaling and the secretion of neurotrophic factors

Marta Sobolczyk-Prawda, Department of Molecular Neurochemistry, Medical University, Lodz, Poland

## Introduction

Lipid rafts, characterized by their enrichment in cholesterol, are dynamic microdomains within the cell membrane. The dynamic nature of lipid rafts can influence the malignant behavior of cancer cells, including disruptions in adhesion and the promotion of aggressive migration and invasion phenotypes. Glioma cells are also known to be sensitive to changes in calcium levels, so investigating compartmentalization may be crucial for understanding glioma development. Particularly, the proposed study may provide new insight into the functional relationship between astrocyte-specific membrane-located GABA transporter 3 (GAT3) and an essential regulator of intracellular  $Ca^{2+}$  concentration, the plasma membrane  $Ca^{2+}$ -ATPase 4 (PMCA4) in C6 glioma cell line.

### AIM:

To investigate the effects of GABA in discrete plasma membrane microdomains and verify whether compartmentalization of these signals may be regulated by plasma membrane  $Ca^{2+}$ -ATPase

## Methods and Results

### Gene expression of SLC6A11 and ATP2B4 is significantly changed in GBM compared with normal

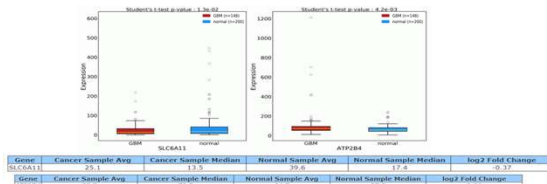


Fig.1. The mRNA level differential expression of SLC6A11 and ATP2B4 from OncoDB server. Orange and blue boxes representing cancerous and normal samples, respectively (results are presented in transcript per million (TPM) unit).

### GAT3 and PMCA4 co-localize in the lipid rafts of C6 cell line

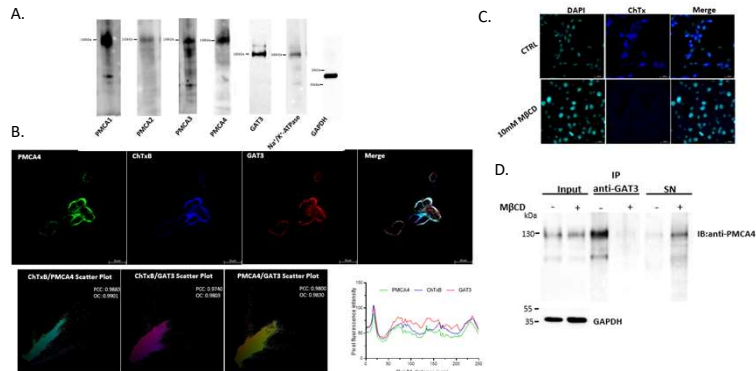


Fig. 2. (A) The presence of the GAT3, and PMCA 1-4 isoforms in the C6 glioma cell line assessed by Western blot. Cells were visualized by inverted-fluorescent microscopy to generate triple co-localization maps. Immunofluorescence of PMCA4 (green), GM1 (lipid rafts marker) labeled with cholera toxin B (ChTxB; blue) and GAT3 (red) in C6 cells. The linear region of interest (ROI) was manually drawn from right to left, and fluorescence intensity profiles were obtained from each individual color channel. Images were analyzed by Pearson coefficient (PC). Scale bar: 20  $\mu$ m. (B) Cells were visualized by inverted-fluorescent microscopy to generate triple co-localization maps. Immunofluorescence of PMCA4 (green), GM1 (lipid rafts marker) labeled with cholera toxin B (ChTxB; blue) and GAT3 (red) in C6 cells. The linear region of interest (ROI) was manually drawn from right to left, and fluorescence intensity profiles were obtained from each individual color channel. Images were analyzed by Pearson coefficient (PC). Scale bar: 20  $\mu$ m. (C) Visualization of lipid rafts (GM1 labeled with ChTxB) in the groups treated and not treated with 10 mM methyl- $\beta$ -cyclodextrin (MBCD) for 1 hour. (D) Immunoprecipitation of GAT3 with PMCA4 in C6 cells treated or untreated with MBCD by 1h (10mM). C6 lysates were immunoprecipitated using GAT3 antibody, separated by SDS-PAGE, and detected by Western blotting using PMCA4 antibody. The supernatant fraction (SN) from each sample was used as a negative control, and next shown by Western blotting using PMCA4 antibody.

### GABA uptake signaling is variably regulated in specific plasma membrane domains by PMCA4

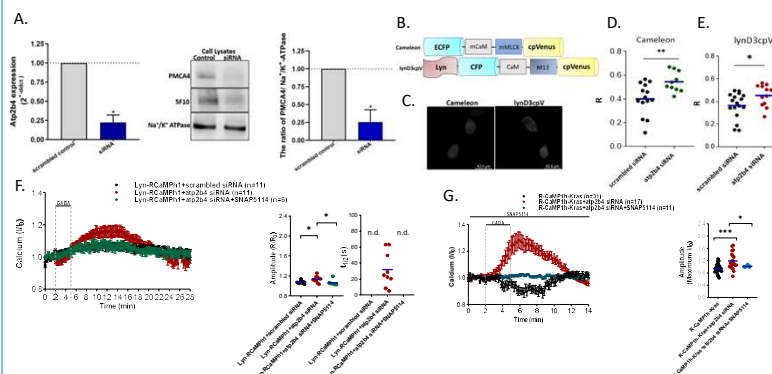


Fig.4. (A) The gene expression level of PMCA4 assessed by real-time PCR. The results are presented as relative units obtained after normalization to GAPDH expression. The level of expression of each target gene in the control line was taken as 1 (dotted line). \*  $p < 0.05$ , siRNA-treated cells vs. control cells. (mean  $\pm$  SD, n = 5). Representative Western blot for PMCA4 protein showing downregulation of PMCA4 by siRNA. In addition, all PMCA4 isoforms were detected with anti-PMCA4 5F10. PMCA4 protein level assessed by densitometric analysis of immunoblots. The results are obtained after normalization to Na<sup>+</sup>/K<sup>+</sup> ATPase level. The dotted line presents the values for control line. \*  $p < 0.05$ , siRNA-treated cells vs. control cells. (mean  $\pm$  SD, n = 3). (B) Scheme of ratiometric Ca<sup>2+</sup> sensor Cameleon and Lyn-D3cpV. (C) Grayscale images of C6 cells expressing these sensors. Scale bar: 42.4  $\mu$ m. Basal [Ca<sup>2+</sup>]<sub>i</sub> (D) and basal [Ca<sup>2+</sup>]<sub>i</sub> at the plasma membrane (E) in siRNA-treated cells vs. control cells. Average tracings of Lyn-RcAMP1h (F) and RCaMP1h-Kras (G) response to 200  $\mu$ M GABA performed for 3 min (horizontal bars) in PMCA4 siRNA- and scrambled siRNA-treated cells, and PMCA4 siRNA-group treated with SNAPS114 inhibitor (25  $\mu$ M). The inhibitor was present throughout the experiment. The amplitude of individual tracings is presented in the scatter plots; blue bars indicate mean. Datasets were compared by unpaired t tests. \*  $p \leq 0.05$ , \*\*\*  $p \leq 0.001$ .

### Long-term exposure to 200 $\mu$ M GABA leads to an increase in [Ca<sup>2+</sup>]<sub>i</sub> in lipid rafts and weakening of the GAT3/PMCA4 complex

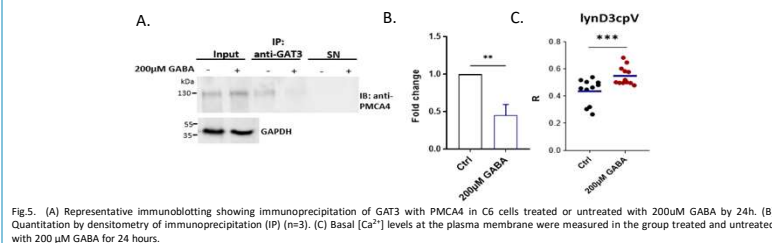


Fig.5. (A) Representative immunoblotting showing immunoprecipitation of GAT3 with PMCA4 in C6 cells treated or untreated with 200  $\mu$ M GABA for 24h. (B) Quantification by densitometry of immunoprecipitation (IP) (n=3). (C) Basal [Ca<sup>2+</sup>]<sub>i</sub> levels at the plasma membrane were measured in the group treated and untreated with 200  $\mu$ M GABA for 24 hours.

### Calcium dynamics in lipid rafts determine the migration and invasive potential of C6 glioma cells

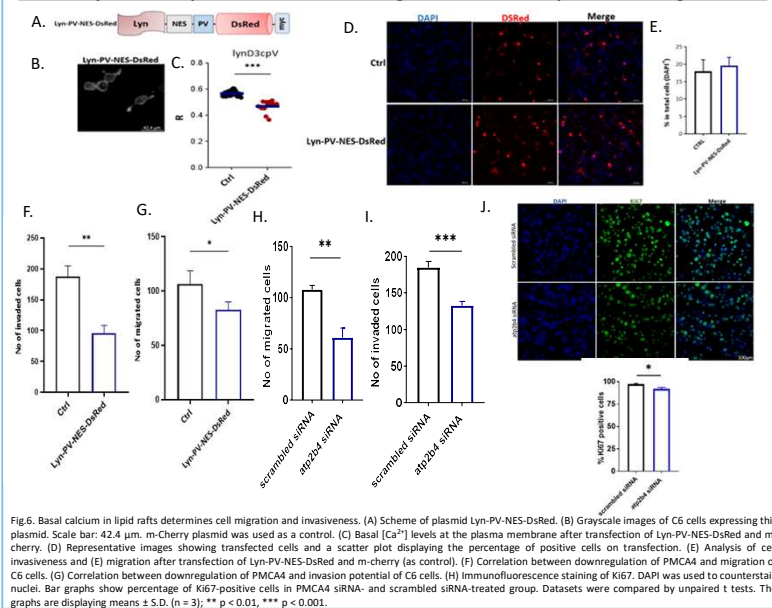


Fig.6. Basal calcium in lipid rafts determines cell migration and invasiveness. (A) Scheme of plasmid Lyn-PV-NES-DsRed. (B) Grayscale images of C6 cells expressing this plasmid. Scale bar: 42.4  $\mu$ m. m-Cherry plasmid was used as a control. (C) Basal [Ca<sup>2+</sup>]<sub>i</sub> levels at the plasma membrane after transfection of Lyn-PV-NES-DsRed and m-cherry. (D) Representative images showing transfected cells and a scatter plot displaying the percentage of positive cells on transfection. (E) Analysis of cell invasiveness and (E) migration after transfection of Lyn-PV-NES-DsRed and m-cherry (as control). (F) Correlation between downregulation of PMCA4 and migration of C6 cells. (G) Correlation between downregulation of PMCA4 and invasion potential of C6 cells. (H) Immunofluorescence staining of Ki67. DAPI was used to counterstain nuclei. Bar graphs show percentage of Ki67-positive cells in PMCA4 siRNA- and scrambled siRNA-treated group. Datasets were compared by unpaired t tests. The graphs are displaying means  $\pm$  S.D. (n = 3); \*\*  $p < 0.01$ , \*\*\*  $p < 0.001$ .

### GABA uptake-mediated Ca<sup>2+</sup> signalling primarily relies on GAT3 and NCX activity

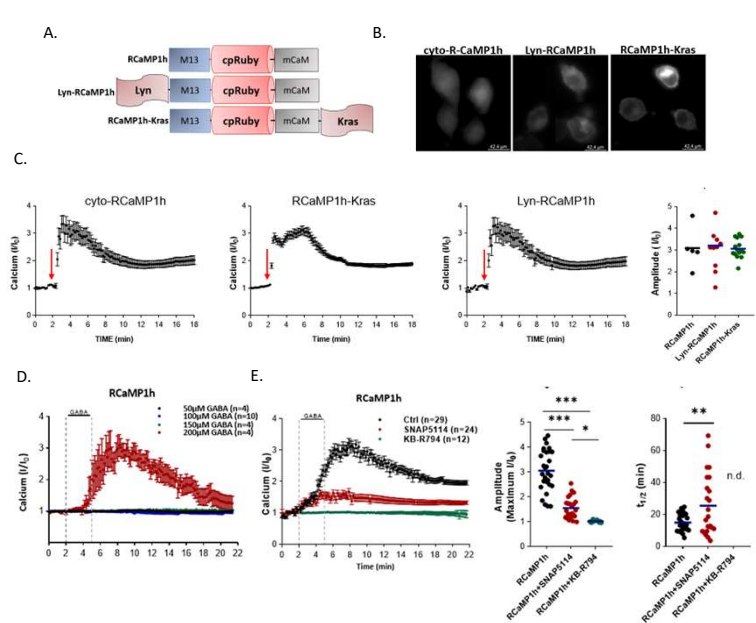


Fig.3. (A) Scheme of intensiometric Ca<sup>2+</sup> sensor RCaMP1h, Lyn-RcAMP1h and RCaMP1h-Kras. Lyn-RcAMP1h is a variant of the RCaMP1h sensor anchoring to lipid rafts of the plasma membrane via myristoylation and palmitoylation. RCaMP1h-Kras is targeted to non-lipid-rafts regions through C-terminal prenylation sequences derived from K-ras (B) Grayscale images of C6 cells expressing RCaMP1h, Lyn-RcAMP1h and RCaMP1h-Kras. Scale bar: 42.4  $\mu$ m. (C) The response of sensors to maximal stimulation. Representative graphs showing the response of sensors to 5  $\mu$ M thapsigargin and 10  $\mu$ M ionomycin to record maximal Ca<sup>2+</sup> response. Arrow indicates drug addition. (D) The response of RCaMP1h sensor to various concentration of GABA. (E) Average tracings (100 $\times$ SEM) depicting the RCaMP1h response to 200  $\mu$ M GABA applied for 3 min in the presence or absence of SNAPS114 (inhibitor of GAT3, 25  $\mu$ M) and KB-R794 (inhibitor of NCX; 10  $\mu$ M). The inhibitors were present throughout the experiment, respectively. The amplitude and half-time of signal decay (1/2) for individual tracings are presented in the scatter plot; blue bars indicate mean. Datasets were compared by unpaired t tests. \*\*  $p < 0.01$ , \*\*\*  $p < 0.001$

## Main conclusions

Visualization of GAT3 demonstrated its predominant location to lipid rafts and a strong colocalization with PMCA4, the main PMCA isoform found in C6 astrocytic cells. Interestingly, GABA-mediated signal transduction is strictly associated with spatial compartmentalization Ca<sup>2+</sup> signal within discrete plasma membrane microdomains. These findings provide new insight into the complex role of membrane microdomains in compartmentalizing calcium signals and their impact on invasiveness potential in an in vitro model of glioma.